



ELSEVIER



CrossMark

journal homepage: www.elsevier.com/locate/febsopenbio

Potential use of potassium efflux-deficient yeast for studying trafficking signals and potassium channel functions[☆]

Joshua D. Bernstein, Yukari Okamoto, Minjee Kim, Sojin Shikano*

Department of Biochemistry and Molecular Genetics, University of Illinois at Chicago, Chicago, IL 60607, USA

ARTICLE INFO

Article history:

Received 18 February 2013

Received in revised form 2 April 2013

Accepted 11 April 2013

Keywords:

Potassium channel

Yeast

Trafficking

Surface membrane

Screening

ABSTRACT

The activity of potassium (K^+) channels critically depends on their density on the cell surface membrane, which is regulated by dynamic protein–protein interactions that often involve distinct trafficking signals on the cargo proteins. In this paper we explored the possibility of utilizing the *Saccharomyces cerevisiae* strain B31 for identification of the signal motifs that regulate surface expression of membrane proteins and for studying structure–function relationships of K^+ channels. B31 cells lack the K^+ efflux system and were reported to show overloaded K^+ -mediated growth inhibition in high K^+ media upon heterologous expression of a mammalian inwardly rectifying K^+ channel (Kir2.1). We show that while the expression of wild-type Kir2.1 channel inhibits the growth of B31 cells in high K^+ media, the human disease-causing mutations of Kir2.1 that abolish K^+ conduction (V302M) or surface trafficking (Δ 314/315) fully restores the growth. The expression of two-pore-domain K^+ channel KCNK3 or KCNK9 also inhibited the growth of B31 in high K^+ media while C-terminal mutations that reduce their 14-3-3 protein-dependent cell surface trafficking restored the growth of B31. Finally, the expression of Kir2.1 channels that were C-terminally fused with known sequence motifs including ER retention/retrieval signals and an endocytosis signal allowed the growth of B31 in high K^+ media. These results demonstrate the potential of B31 yeast strain as a unique biological tool to screen the random peptide libraries for novel sequence signals that down-regulate surface expression of membrane proteins, as well as to systematically identify the structural determinants for cell surface trafficking and/or ion conductance of K^+ channels.

© 2013 The Authors. Published by Elsevier B.V. on behalf of Federation of European Biochemical Societies. All rights reserved.

1. Introduction

Ion channels play crucial roles in the cellular response to signals and changes in the extracellular environment by controlling ion homeostasis and membrane excitability. Their proper functioning critically depends on the fine tuning of their localization at cell surface. This process is dictated by the secretory and endocytic vesicular trafficking pathways that often involve dynamic interactions between distinct sequence signals on the cargos and cellular transport machineries. Many important discoveries on trafficking signals have come from the studies on ion channels including K^+ channels. For instance, the Arg-based ('RXR') endoplasmic reticulum (ER) retention/

retrieval signal was first discovered in the ATP-sensitive inwardly rectifying K^+ channel (Kir) subunit, Kir6.2 [1]. This finding has led to a proposed mechanism by which the incompletely assembled channel proteins can be screened for a distinct peptide signal by the quality control system and returned to the ER. The RXR motif is recognized by a coatomer protein (COP) complex that forms the Golgi-to-ER retrograde transport vesicles [1–3], and now numerous surface membrane proteins including ion channels and receptors are known to carry this signal [4–7]. Moreover, multiple different peptide signals necessary for promoting cell surface trafficking have been also found in K^+ channels [8–11]. These findings have supported a concept that the surface trafficking of membrane proteins is not a default process but is highly regulated by different sequence motifs that are displayed on the cargo proteins.

Yeast offers a good model for studying mammalian protein trafficking mechanisms, since basic molecular machinery for protein trafficking is well conserved between yeast and mammals. More importantly, clonal expression of library transgenes in a cell enables a systematic screening and analysis, which is not achievable in mammalian cells that will inevitably take up multiple gene clones within a cell upon transfection of libraries. The ability of animal K^+ channels

[☆] This is an open-access article distributed under the terms of the Creative Commons Attribution License, which permits unrestricted use, distribution, and reproduction in any medium, provided the original author and source are credited.

Abbreviations: ER, endoplasmic reticulum; FCM, flow cytometry; COP, coatomer protein; IP, immunoprecipitation; Ab, antibody; HA, hemagglutinine; SD, standard deviation; aa, amino acids; O/N, overnight

* Corresponding author. Address: 900 S. Ashland Ave, MBRB2006, Chicago, IL 60607, USA. Tel.: +1 312 413 2029; fax: +1 312 413 0353.

E-mail address: sshikano@uic.edu (S. Shikano).

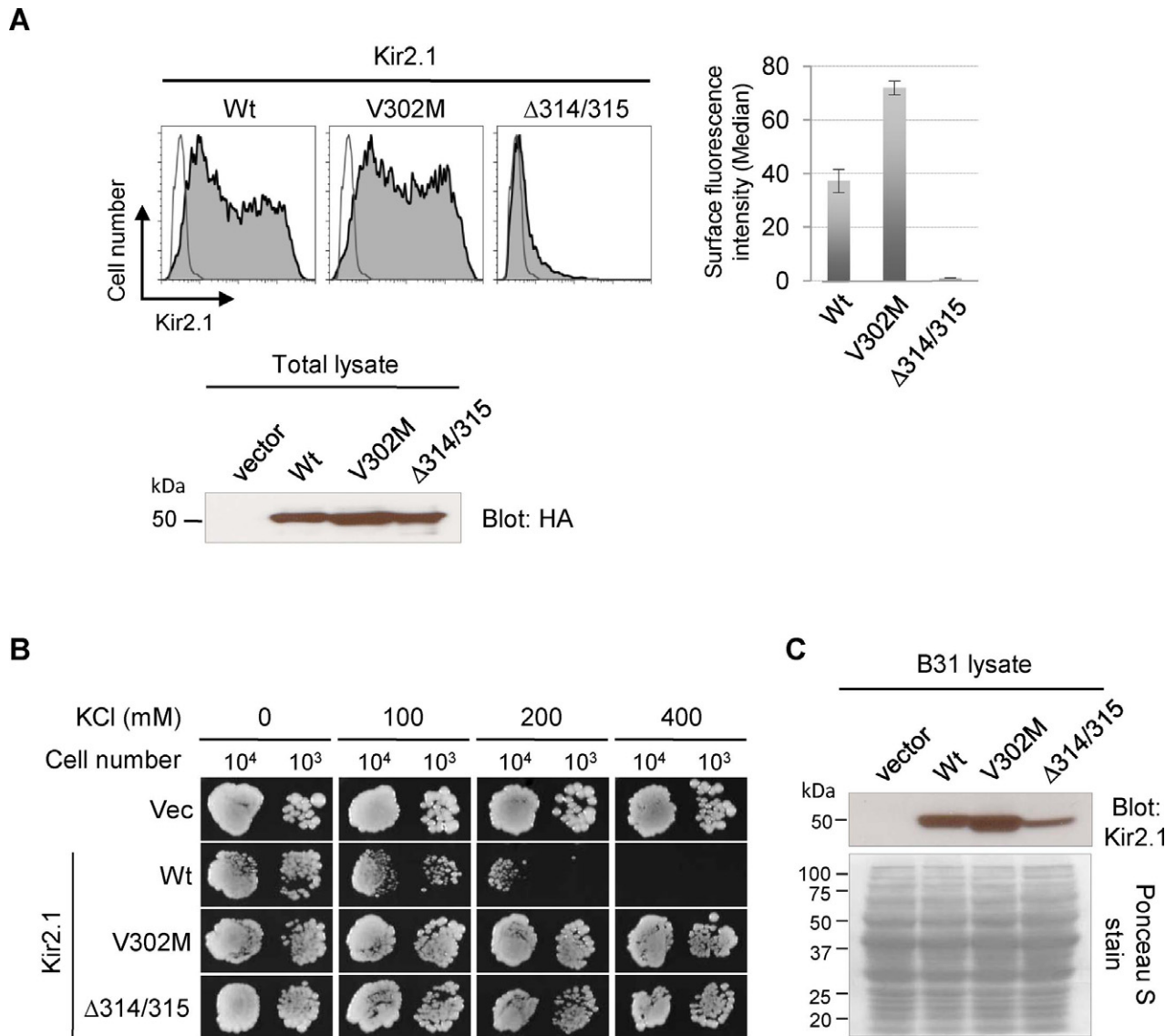


Fig. 1. B31 tolerance to high K^+ media represents the loss of Kir2.1 activity on cell surface. (A) Surface expression of Kir2.1 channels. HEK293 cells were transiently transfected with HA-tagged Kir2.1 constructs or pCDNA3.1(+) vector alone. Cells stained with the HA Ab followed by Alexa Fluor 488-conjugated secondary Ab were analyzed by flow cytometry (FCM). Histograms from the representative samples are shown (left panels). The x-axis indicates the fluorescence intensity in a logarithmic scale and y-axis indicates the cell number. The histograms of Kir2.1-transfected cells (filled) were overlaid with that of vector-transfected cells (unfilled). The bar graph (right panel) shows the Median values for the total cell populations determined by FlowJo software to compare the relative surface intensity of Wt and mutant Kir2.1 channels. The values indicate average \pm s.d. of triplicate samples from the representative of three experiments. The lower panel shows the total expression levels of Kir2.1 proteins. Total lysates from HEK293 cells transfected with HA-Kir2.1 constructs were resolved by SDS-PAGE and immunoblotted for HA. (B) Growth assay of Kir2.1-expressing B31. The Kir2.1- or pYES2met vector-transformed B31 cells were plated on YNB media (pH 6.50) with the indicated concentrations of KCl and cultured at 30 °C. The images were photographed at Day 5. (C) Expression of Kir2.1 channels in B31 cells. The proteins were extracted from B31 cells transformed with pYES2met vector or the indicated Kir2.1 constructs. The samples were resolved by SDS-PAGE and immunoblotted for Kir2.1 (upper panel). The lower panel shows the Ponceau S staining of the transfer membrane, indicating similar loading of the proteins for each sample.

such as Kir family channels to complement the growth of K^+ uptake-deficient *Saccharomyces cerevisiae* strain, e.g., SGY1528 that lacks K^+ uptake transporters Trk1 and Trk2 [12], in low K^+ media has proven particularly useful for identification of novel trafficking pathways of membrane proteins. For instance, Shikano et al. used SGY1528 cells to screen library of Kir2.1 channels that are fused with C-terminal random 8-mer peptide sequences and identified a group of *cis*-acting sequences that specifically interact with 14-3-3 proteins and promote surface expression of membrane proteins [13]. Moreover, the screening of a cDNA library transduced into the Kir2.1 channel-expressing SGY1528 cells resulted in a discovery of a *trans*-acting protein that enhances the cell surface expression of Kir2.1 [14]. The SGY1528 has been also successfully used to identify the structural determinants for the K^+ selectivity of G-protein gated inwardly-rectifying K^+ channel

(GIRK) [15].

On the other hand, Kolacna and colleagues have developed K^+ efflux-deficient *S. cerevisiae* strain, B31. This strain lacks a Na^+ -ATPase and a Na^+ / H^+ antiporter and therefore shows growth inhibition in high K^+ media due to the excessive accumulation of intracellular K^+ upon heterologous expression of a mammalian Kir2.1 channel [16]. Having the fact that Kir2.1 activity inversely correlates with the B31 growth in high K^+ , we explored the possibility that B31 growth assay can be conveniently utilized to systematically screen for the structural determinants of K^+ channel functions and for the novel signal motifs that down-regulate cell surface expression of membrane proteins by a gain-of-function (i.e., cell survival) assay. As a proof of concept, we examined (1) if specific mutations that disrupt functions of Kir2.1 can be represented by B31 tolerance to high K^+ , (2) if other

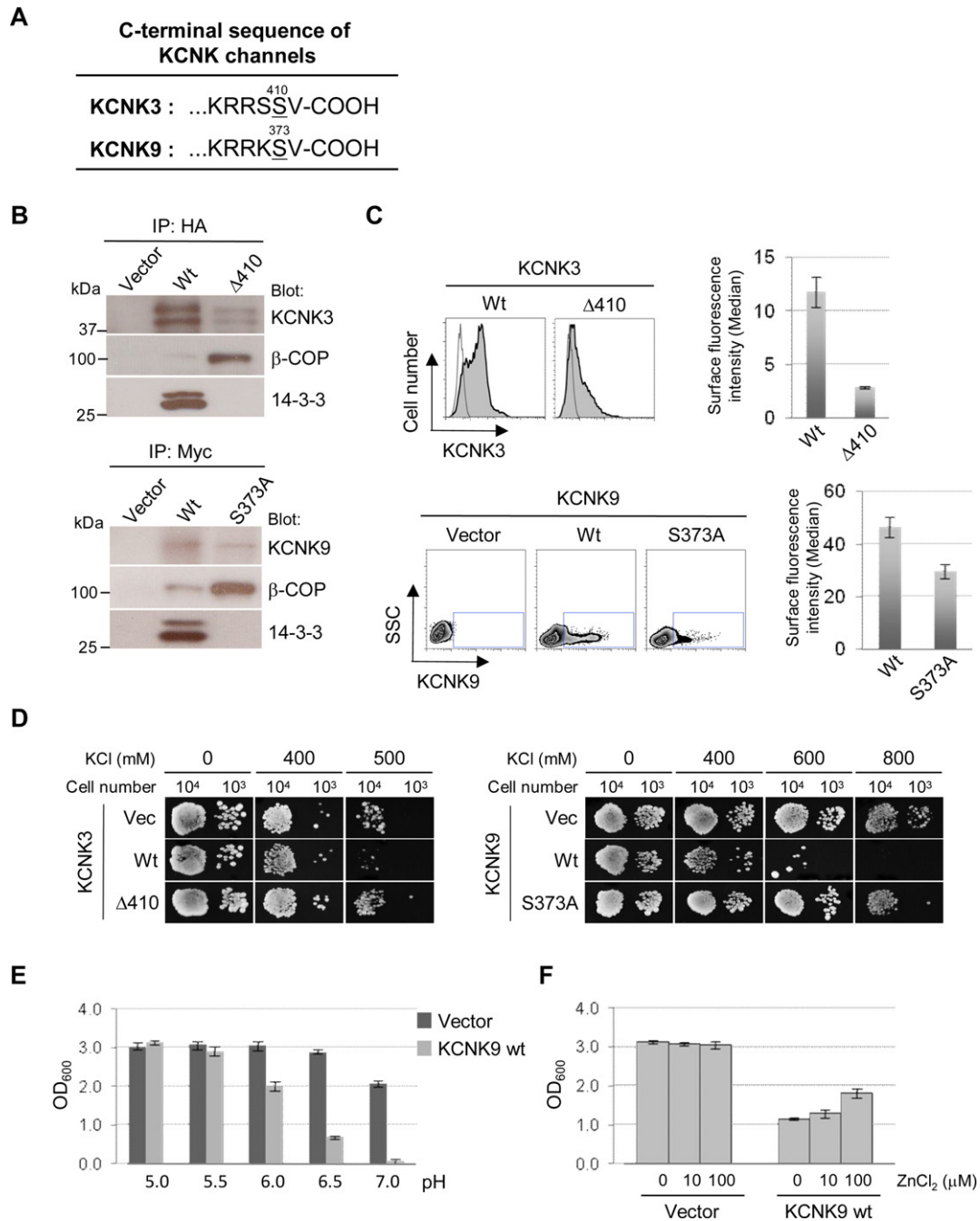


Fig. 2. B31 growth inhibition in high K^+ media represents KCNK channel activities on cell surface. (A) Alignment of C-terminal sequences from KCNK3 and KCNK9 channels. (B) Association of COPI and 14-3-3 proteins with KCNK3 (upper panels) and KCNK9 (lower panels). HEK293 cells transfected with HA-KCNK3 or Myc-KCNK9 were lysed and immunoprecipitated with HA or Myc Abs. The eluants were resolved by SDS-PAGE and immunoblotted for the associating β -COP and 14-3-3 as well as HA (KCNK3) or Myc (KCNK9). (C) Surface expression of KCNK3 and KCNK9. HEK293 cells were transfected with HA-tagged rat KCNK3 or Myc-tagged human KCNK9 and analyzed for cell surface expression by FCM. For KCNK3 (upper panels), the expression is shown in histograms and the Median values were determined for the total cell populations as described for Fig. 1. The histograms of KCNK3-transfected cells (filled) were overlaid with that of vector-transfected cells (unfilled). For KCNK9 (lower panels), the expression is shown in density plots (see Section 2) where x-axis indicates the fluorescence intensity in a logarithmic scale and y-axis indicates the side scatter (SSC) of the cell. The Median values were determined for the cells that were positive for the KCNK9 signal (shown in squares within the density plots). The bar graphs indicate the Median values in average \pm s.d. of triplicate samples from the representative of three different experiments. (D) Growth assay of KCNK-expressing B31. The KCNK- or pYES2met vector-transformed B31 cells were plated on YNB media (pH 7.0 for KCNK3 and pH 6.50 for KCNK9) with indicated concentrations of KCl and cultured at 30 °C. The images were photographed at Day 7. (E) The effect of pH on the growth of KCNK9-expressing B31. The B31 cells transformed with vector or KCNK9 Wt were grown in the liquid YNB media with indicated pH and 400 mM KCl. (F) The effect of zinc on the growth of KCNK9-expressing B31. The B31 cells transformed with vector or KCNK9 Wt were grown in the liquid YNB media with indicated concentrations of $ZnCl_2$ and 400 mM KCl at pH 6.50. In both of the pH and zinc tests, the OD at 600 nm was measured at the start of and after 15 h of culture. The values after the culture was subtracted with those at the start and shown in average \pm s.d. of triplicate samples from the representative of three experiments.

K⁺ channel family members can also function in B31 growth assay, and (3) if the activities of Kir2.1-fused trafficking signals that down-regulate surface expression can be represented by B31 tolerance to high K⁺.

2. Materials and methods

2.1. Plasmids

For B31 growth assay, mouse Kir2.1 was cloned at BamHI and NotI in pYES2 vector in which GAL1 promoter was replaced with MET25 promoter (kindly supplied by Dr. Lily Jan). The EcoRI site was added before the termination codon (this was referred to as a wild-type Kir2.1) for fusion of the exogenous trafficking motifs. The C-terminal sequences were cloned from mouse Kir6.2 (aa 355–399), human GPR15 (aa 351–360), or human sodium-dependent dopamine transporter [17] (aa 587–596) and fused to Kir2.1 at EcoRI-NotI. For GPR15 sequence, Ser residue at 359 was mutated to Ala. Human KCNK3 and KCNK9 were also cloned in pYES2met vector. Site-directed mutagenesis was performed by overlap extension PCR. For detection of cell surface expression in HEK293 cells, Kir2.1 was tagged with hemagglutinin (HA) epitope at between aa 117 and 118, rat KCNK3 was tagged with HA at between aa 213 and 214, and human KCNK9 was tagged with Myc between aa 40 and 41. These tagged constructs were cloned in pCDNA3.1(+) vector (Invitrogen, Carlsbad, CA).

2.2. Yeast strains and growth conditions

The *S. cerevisiae* strain B31 (*MAT α ena1-4::HIS3 nha1::LEU2*) is a derivative of W303-1A (*MAT α ade 2-1 can1-100 his3-11/15 leu2-3/112 mal10 trp1-1 ura3-1*) [16] and was kindly provided by Dr. Hana Sychrova. Cells were grown aerobically at 30 °C on YPD (1% yeast extract, 2% bactopectone, 2% glucose, 120 mg/L adenine hemisulfate, 1.7% agar for solid media) or YNB media (6.7 g/L yeast nitrogen base without amino acids, 2% glucose, 10 mg/L adenine hemisulfate, 0.73 g/L methionine- and uracil-dropout amino acid mixture, 1% agar for solid media). The YNB media were supplemented with the indicated amount of potassium chloride and adjusted to pH 6.5 or 7.0 by Tris-HCl.

2.3. Plasmids and yeast transformation

Yeast cells grown to early logarithmic phase in YPD media were transformed by a lithium acetate method [18] and plated on YNB plates with no additional KCl (referred to as 0 mM K⁺ plate).

2.4. Growth assay of B31

For the growth assay of the K⁺ channel-transformed B31 cells, the cells were taken from the isolated colonies of freshly-transformed B31 cells and adjusted to 2×10^6 cells/ml in water by using a hemocytometer. This was followed by two 10-fold serial dilutions and 5 μ l aliquots of each dilution were spotted on the YNB plates with indicated concentrations of KCl. Plates were incubated at 30 °C and the digital images of the cells were taken at the indicated times (usually Days 5–7).

2.5. Growth assay of KCNK9-expressing B31 in liquid media

For testing the effect of pH on B31 growth, the cells freshly transformed with pYes2met vector or Wt KCNK9 were adjusted to 2×10^6 cells/ml in YNB media (400 mM KCl) with pH adjusted to 5.0, 5.5, 6.0, 6.5, or 7.0 using Tris-HCl. For testing the effect of zinc ion, the cells were adjusted as above in YNB media (400 mM KCl, pH 6.5) containing 0, 10, and 100 μ M zinc chloride. Zinc chloride at higher than 100 μ M caused salt precipitation and reduction of the medium pH, so

was not tested. The turbidity (OD 600 nm) was measured before and after 15 h of culture at 30 °C. Cultures were performed in triplicate for each construct.

2.6. Antibodies (Abs)

The following Abs were used: mouse HA, rabbit Kir2.1, and rabbit 14-3-3 β from Santa Cruz Biotechnologies (Dallas, TX), rabbit HA from Cell Signaling Technology (Danvers, MA), mouse Myc (both non-conjugated and Alexa Fluor (AF) 488-conjugated) from Millipore (Billerica, MA), rabbit β -COP from Affinity BioReagent (Golden, CO), mouse GST from NeuroMab (Davis, CA), AF488-conjugated goat anti-mouse IgG from Invitrogen, horse radish peroxidase (HRP)-conjugated goat anti-mouse and goat anti-rabbit IgG from Vector laboratory (Berlingame, CA).

2.7. Cell culture and transfection

HEK293 cells were maintained in 50% DMEM/50% Ham's F-12 medium containing 10% FBS, 2 mM L-glutamine, 100 U/ml penicillin, and 100 μ g/ml streptomycin. Transient transfection of plasmids was performed using Mirus TransIT-LT1 (Mirus Bio, Madison, WI) according to the manufacturer's instructions.

2.8. Flow cytometry (FCM)

Transfected HEK293 cells were collected by gentle flushing and washed with Hanks' Balanced Salt Solution supplemented with 1% BSA (staining buffer). All the Ab staining and washing thereafter were performed in the staining buffer on ice. For surface staining of HA-tagged Kir2.1 and KCNK3, the transfected cells were incubated with mouse HA Ab followed by AF488-conjugated secondary Ab for 20 min on ice. For Myc-tagged KCNK9, the transfected cells were stained with AF488-conjugated mouse Myc Ab. The stained cells were fixed with 1% paraformaldehyde and analyzed by Cell Lab Quanta SC (Beckman Coulter, Brea, CA). For measurement of surface fluorescence intensity, the Median values were determined for the entire cell populations (Kir2.1 and KCNK3) or for the myc-positive population (KCNK9) by using FlowJo software (Tree Star Inc., Ashland, OR). The surface expression of the channels was shown in the histograms except that KCNK9 expression was shown in a density plot because the percentage of KCNK9 signal-positive cells were too small (<10%) to clearly show in histograms. This may be due to the inefficient accessibility of the Myc Ab to the epitope.

2.9. Protein extraction from B31 yeast cells

Proteins were extracted from B31 cells to examine the expression of Kir2.1 channels. B31 cells transformed with pYES2met vector or Kir2.1 constructs were inoculated in the methionine- and uracil-deficient YNB media with no added KCl and cultured O/N at 30 °C. The next morning the cell density was adjusted to a density of 0.3 OD600 in 3 ml of the same medium and cultured for 4 h. The proteins were extracted as described previously [19] and the samples were subjected to the western blot for Kir2.1 and KCNK channels.

2.10. Immunoprecipitation (IP)

The transfected HEK293 cells were washed with PBS once and lysed with lysis buffer (0.5% Igepal, 25 mM Tris, 150 mM NaCl, pH 7.5) containing protease inhibitors for 20 min at 4 °C. After centrifugation for 20 min at 11,000xg, the supernatant was mixed with mouse HA or mouse Myc and Protein A- or Protein G-conjugated agarose beads (Invitrogen). After O/N incubation at 4 °C, the beads were washed 4 times with lysis buffer and then the immunoprecipitated proteins were eluted by incubating the beads with 2X sample buffer.

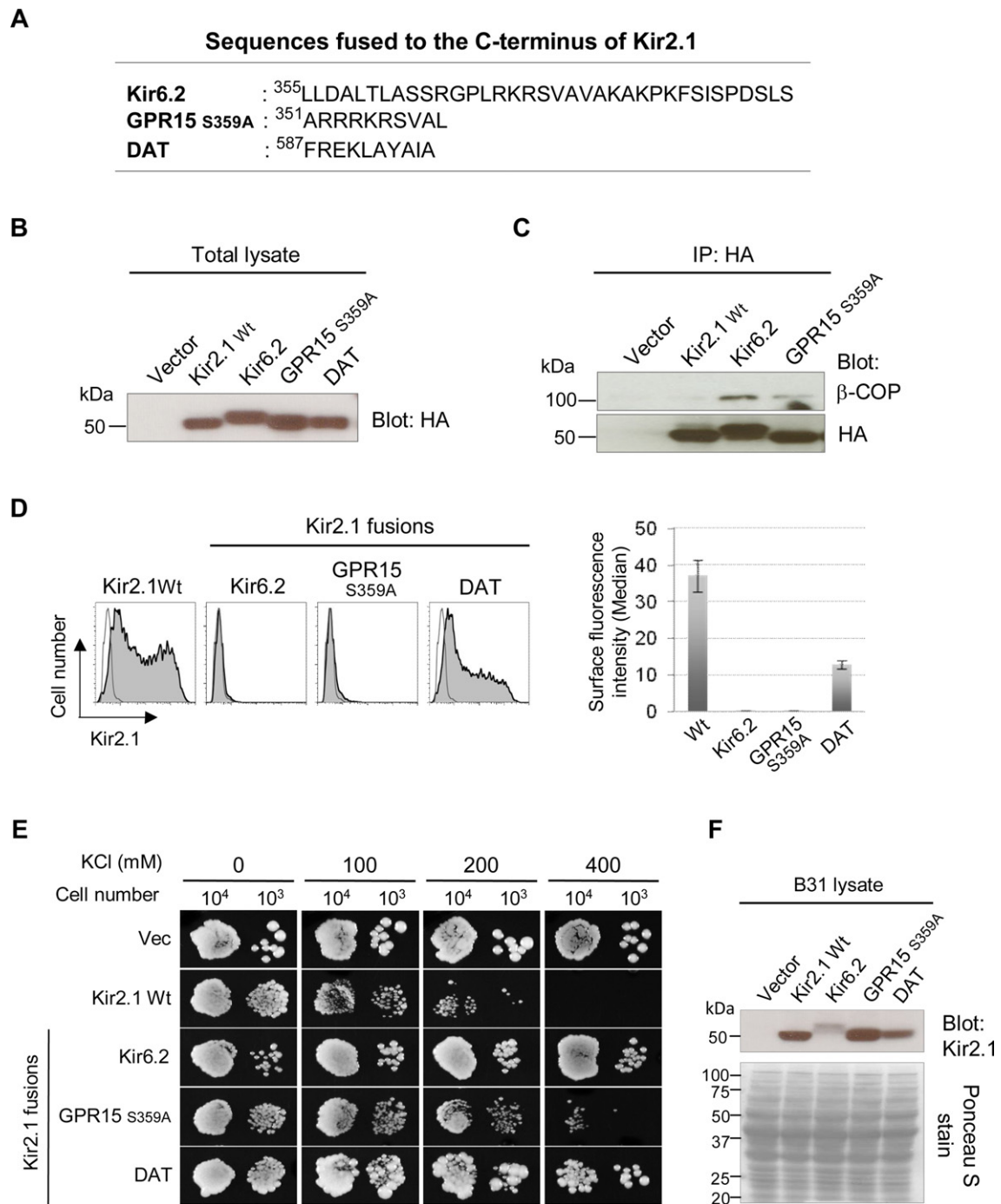


Fig. 3. B31 tolerance to high K^+ represents the activity of trafficking signals that down-regulate surface expression of membrane proteins. (A) Sequences that were fused to the C-terminus of Kir2.1 channels. (B) Total expression levels of Kir2.1 fusions. Total lysates from HEK293 cells transfected with HA-Kir2.1 constructs were resolved by SDS-PAGE and immunoblotted for HA. (C) Association of COPI with Kir2.1 fusions. The Kir2.1 fusions immunoprecipitated with HA Ab were resolved by SDS-PAGE and immunoblotted for HA (lower panel) and the associating β -COP (upper panel). (D) Surface expression of Kir2.1 fusions. HEK293 cells were transfected with HA-Kir2.1 constructs and analyzed for cell surface expression by FCM. The histograms (left panels) of Kir2.1-transfected cells (filled) were overlaid with that of vector-transfected cells (unfilled). The Median values were determined for the total cell populations and shown in average \pm s.d. of triplicate samples from the representative of three experiments (right panel). (E) Growth assay of B31 expressing Kir2.1 fusions. The Kir2.1- or pYES2met vector-transformed B31 cells were plated on YNB media (pH 6.50) with indicated concentrations of KCl and cultured at 30 °C. The images were photographed at Day 7. (F) Expression of Kir2.1 channels in B31 cells. The proteins were extracted from the B31 cells transformed with pYES2met vector or the indicated Kir2.1 constructs. The samples were resolved by SDS-PAGE and immunoblotted for Kir2.1 (upper panel). The lower panel shows the Ponceau S staining of the transfer membrane, indicating similar loading of the proteins for each sample.

2.11. SDS-PAGE and western blots

The protein samples resolved by 10 or 12% SDS-PAGE were transferred to nitrocellulose membranes. Transfer was confirmed by staining of the membranes with Ponceau S. The membranes were blocked with skim milk and then incubated with primary Abs for 1 h at room temperature (RT) or O/N at 4 °C and then with corresponding secondary Abs conjugated with HRP. Blot signals were obtained using ECL substrates (Thermo Scientific) and collected by exposure to X-ray films.

3. Results and discussion

3.1. B31 tolerance to high K^+ media represents the loss of Kir2.1 activity on cell surface

A previous study by Kolacna et al. reported that B31 strain (*ena1-4Δ nha1Δ*) lacking the K^+ and Na^+ efflux system shows sensitivity to higher external concentrations of alkali-metal-cation salts when transformed with a mammalian Kir2.1 channel [16]. We explored the potential of B31 cells as a tool for identifying the structural determinants of Kir2.1 channel functions by testing the mutants of Kir2.1. We selected V302M and Δ 314/315 mutants, which are both responsible for human Andersen-Tawil syndrome that causes periodic paralysis and ventricular arrhythmias [20]. The V302M mutation is reported to disrupt K^+ ion conduction through G-loop without reducing the cell surface expression of the channel [21], while Δ 314/315 (deletion of aa 314 and 315) is known to retain the channel in the Golgi [20,22]. Our flow cytometry (FCM) and western blot analyses of the transfected HEK293 cells confirmed the cell surface phenotypes of these mutant Kir2.1 channels (Fig. 1A). Slightly elevated surface expression of V302M mutant compared with the wild-type (Wt) Kir2.1 was consistent with the observations from other studies [21]. On this basis, we tested the growth of B31 cells transformed with these Kir2.1 constructs. Consistent with the previous report [16], the expression of Wt Kir2.1 showed a marked growth inhibition of B31 cells in high external KCl conditions such as 200 mM and higher (Fig. 1B, 2nd row). In contrast, both of the mutants V302M and Δ 314/315 allowed growth of B31 at comparable level to that of vector-transformed cells (Fig. 1B, 1st, 3rd, and 4th rows). In B31 yeast cells, the Δ 314/315 mutant channel showed somewhat lower expression than Wt and V302M channels did (Fig. 1C). This may represent possibly higher susceptibility of the intracellularly retained Kir2.1 channels to the proteolytic pathways in yeast, relative to the surface trafficking-competent channels.

It is conceivable that other inwardly rectifying channel family members also work in a similar manner to that of Kir2.1. Thus, combined with random mutagenesis techniques such as an error-prone PCR, the B31 growth assay will enable a systematic screening to identify the functional determinants of Kir channels, in which the loss of channel activity at cell surface can be conveniently visualized as yeast cell survival. The recently reported improvement in yeast transformation efficiency [23] may further promise success of such assays.

3.2. B31 growth inhibition in high K^+ media represents KCNK channel activities on cell surface

We were curious if other K^+ channel family members can also be studied in B31 yeast. It has been reported that a voltage-gated mammalian neuronal K^+ channel *ether à go-go 1* (EAG1), when lacking its intracellular N-terminus, can be functionally expressed in B31 and increase the growth sensitivity to high K^+ [24]. It is conceivable that a K^+ channel with high open probability at the resting membrane potential has a good chance to function in B31 cells. We tested two members of a two-pore-domain K^+ channel (KCNK) family, KCNK3 and KCNK9. Many of the KCNK family members are open channels

and responsible for generating the background 'leak' K^+ current at the resting membrane potential [25]. Increasing studies show critical involvement of KCNK channels in a wide range of human diseases. For instance, human genetic studies indicate an involvement of KCNK3 gene in the pathogenesis of primary hyperaldosteronism [26]. KCNK9 was found to be overexpressed in various human cancers and its overexpression was experimentally shown to be sufficient to confer a tumorigenic phenotype such as tolerance to low oxygen and low serum [27]. In addition, a genetic point mutation of KCNK9 is associated with abnormal development that causes a mental retardation [28]. Nevertheless, compared with other voltage-gated K^+ channel families, KCNKs are still relatively new and their biochemical properties are not fully understood.

Previous studies including ours reported that KCNK3 and KCNK9 channels carry a 14-3-3 protein binding motif at the extreme C-terminus (RXXSX-COOH, see Fig. 2A) [6,13]. The phosphorylation-dependent 14-3-3 binding appears to occlude the overlapping di-basic ER retention/retrieval signal that would be otherwise recognized by the COPI complex, and thus allows optimal surface trafficking of the channels. The presence and the exact penultimate position of the Ser residue (Fig. 2A underlined) in the C-terminus is critical for the 14-3-3 binding [6,13]. So, we created the 14-3-3 binding-deficient KCNK channels by shifting the position of a penultimate Ser (KCNK3 Δ 410) or by mutating Ser to Ala (KCNK9 S373A). These mutants and Wt channels were expressed in HEK293 cells and examined for the association with 14-3-3 and COPI proteins (Fig. 2B). As expected, both KCNK3 and KCNK9 mutants lacked 14-3-3 binding but associated with more β -COP, a major binding subunit of COPI complex, than the Wt channels did. The FCM analysis showed that the surface expression of these mutants were substantially lower when compared with that of Wt channels (Fig. 2C). Having this, we expressed these KCNK channels in B31 for the growth test (Fig. 2D). The expression of Wt KCNK3 and Wt KCNK9 resulted in a marked growth inhibition of B31 cells on the high external K^+ plates, i.e., 500 mM for KCNK3 (left panels) and 600 mM for KCNK9 (right panels). In contrast, the 14-3-3-binding mutants allowed similar level of growth to that of vector-transformed cells. The expression of KCNK proteins in these B31 transformants was below detectable level by the antibodies we used (data not shown). Wt KCNK9 also caused substantial inhibition of B31 growth in the liquid media with high K^+ , and this inhibition was sensitive to the acidic pH lower than 6.0 (Fig. 2E). This was consistent with the reported acid sensitivity of several KCNK members including KCNK9 [25]. Moreover, the growth inhibition of KCNK9-transformed B31 was attenuated by zinc ion (Fig. 2F), which has been reported to inhibit this channel in mammalian cell [29]. These results indicate that KCNK3 and KCNK9, and possibly more KCNK members, function in B31 yeast similarly to Kir2.1 to confer sensitivity to high external K^+ . Thus, B31 growth assay offers a valuable tool for identifying the structural determinants for the activities and cell surface expression of KCNK channels. Moreover, the restored growth of KCNK9-transformed B31 in liquid culture with zinc (Fig. 2F) provides a basis for potential high-throughput screening for small molecule inhibitors of KCNK channels. Indeed, such work has been reported with SGY1528 strain to successfully identify the inhibitors of Kir2.1 channel [30].

3.3. B31 tolerance to high K^+ represents the activity of trafficking signals that down-regulate surface expression of membrane proteins

The utility of K^+ transport-defective yeast is not limited to the study of K^+ channel biology itself. We previously used the K^+ uptake-deficient strain SGY1528 to screen a random peptide library for the novel signal motifs that would promote cell surface trafficking of membrane proteins [13]. The Kir2.1 channels fused with 8-mer random peptide library sequences at the C-terminus were transformed in SGY1528 and screened for the clones that promoted cell growth in

low external K^+ media. This screen identified the C-terminal 14-3-3 binding motifs that were eventually found to promote surface expression of various membrane proteins including a G-protein coupled receptor GPR15 as well as KCNK3 and KCNK9 channels [4,13]. Since the loss of cell surface Kir2.1 or KCNK channels results in B31 survival in high K^+ media (Figs. 1 and 2), we thought that B31 strain would be potentially applicable to such screening of the random peptide library that would allow identification of novel sequence motifs that down-regulate surface expression of membrane proteins. To explore this possibility we tested the signal motifs that have been reported to target intracellular compartments. These include the RXR-type ER retention/retrieval motifs from the C-terminus of Kir6.2 channel [1] and a G-protein coupled receptor GPR15 [4], and also the endocytosis motif from a dopamine transporter DAT [17] (Fig. 3A). For the RXR motif from GPR15, the penultimate Ser was mutated to Ala (S359A) in order to prevent occlusion of the RXR motif (Arg³⁵²/Arg³⁵⁴) by 14-3-3 binding [4]. The expression levels of these Kir2.1 fusions were similar in the transiently transfected HEK293 cells (Fig. 3B). As expected, the Kir2.1 fused with the RXR motifs from Kir6.2 and GPR15_{S359A} were associated with more β -COP when compared with Wt Kir2.1 (Fig. 3C). The FCM analysis showed that the surface expression of all of the tested Kir2.1 fusions were significantly lower than that of Wt channel (Fig. 3D). Then we addressed if these cell surface phenotypes of Kir2.1 channels are represented by the B31 growth. All of the Kir2.1 fusions allowed better growth of B31 in high K^+ media when compared with Wt Kir2.1 (Fig. 3E). In B31 cells, the Kir2.1 channels fused with the RXR motif from Kir6.2 and the endocytic motif from DAT showed somewhat lower expression than the Wt channel did (Fig. 3F). As mentioned for the Kir2.1 Δ 314/315 mutant (Fig. 1C), we believe that this represents the enhanced susceptibility of those channels to the yeast degradation pathways due to their intracellular retention. It is of note that the RXR motif from GPR15_{S359A} did not support B31 growth as efficiently as the RXR motif from Kir6.2 did (Fig. 3E), while both of these motifs seemed equally effective in retaining the Kir2.1 channel in HEK293 cells (Fig. 3D). In addition, the endocytic motif from DAT was less effective in reducing the surface expression of Kir2.1 in HEK293 cells while it allowed more B31 growth when compared with the GPR15_{S359A} sequence. These observations might reflect the difference between yeast and mammalian cells in the recognition of these trafficking motifs by the cellular transport machineries. Nevertheless, our results indicate that the C-terminally transplanted signal motifs attenuated the Kir2.1 channel activity by reducing its cell surface density in B31 yeast. This demonstrate the potential of B31 strain for identifying the *cis*-acting peptide sequences that down-regulate surface trafficking of the K^+ channels and other membrane proteins in mammalian cells.

Although the RXR motifs have been found in increasing number of surface membrane proteins [4–7], their physiological roles and biochemical characteristics are still not fully understood. Moreover, certain proteins are known to use COPI-independent retrograde transport [31,32], which implies the presence of unidentified pathways that regulate cell surface expression. In addition, in spite of extensive studies on the endocytic motifs such as those interact with clathrin adaptors [33], novel motifs that mediate internalization of surface membrane proteins continue to be discovered [34,35]. Hence, the functional screening of the random peptide libraries in B31 will be a promising approach to elucidate novel trafficking mechanisms of membrane proteins. Since the activity of trafficking motifs would depend on the structural attributes of the protein in which they are placed, identification of more K^+ channels that function in B31 cells will increase the chance of success in such screens.

Acknowledgements

We are thankful to Dr. Hana Sychrova of Academy of Sciences of the Czech Republic for providing B31 strain. This study was supported by National Institutes of Health Grant 1R01GM099974–01 (to S.S.) and LUNgevity Foundation/American Cancer Society Lung Cancer Research Grant 2009–07001–00–00 (to S.S.).

References

- [1] Zerangue N., Schwappach B., Jan Y.N., Jan L.Y. (1999) A new ER trafficking signal regulates the subunit stoichiometry of plasma membrane K(ATP) channels. *Neuron* 22, 537–548.
- [2] Michelsen K., Schmid V., Metz J., Heusser K., Liebel U., Schwede T. et al. (2007) Novel cargo-binding site in the beta and delta subunits of coatamer. *J. Cell Biol.* 179, 209–217.
- [3] Popoff V., Adolf F., Brugger B., Wieland F. (2011) COPI budding within the Golgi stack. *Cold Spring Harb. Perspect. Biol.* 3, a005231.
- [4] Okamoto Y., Shikano S. (2011) Phosphorylation-dependent C-terminal binding of 14-3-3 proteins promotes cell surface expression of HIV co-receptor GPR15. *J. Biol. Chem.* 286, 7171–7181.
- [5] Hegedus T., Aleksandrov A., Cui L., Gentzsch M., Chang X.B., Riordan J.R. (2006) F508del CFTR with two altered RXR motifs escapes from ER quality control but its channel activity is thermally sensitive. *Biochim. Biophys. Acta* 1758, 565–572.
- [6] O'Kelly I., Butler M.H., Zilberberg N., Goldstein S.A. (2002) Forward transport, binding overcomes retention in endoplasmic reticulum by dibasic signals. *Cell* 111, 577–588.
- [7] Zhang Z.N., Li Q., Liu C., Wang H.B., Wang Q., Bao L. (2008) The voltage-gated Na^+ channel Nav1.8 contains an ER-retention/retrieval signal antagonized by the beta3 subunit. *J. Cell Sci.* 121, 3243–3252.
- [8] Yoo D., Fang L., Mason A., Kim B.Y., Welling P.A. (2005) A phosphorylation-dependent export structure in ROMK (Kir 1.1) channel overrides an endoplasmic reticulum localization signal. *J. Biol. Chem.* 280, 35281–35289.
- [9] Ma D., Zerangue N., Lin Y.F., Collins A., Yu M., Jan Y.N. et al. (2001) Role of ER export signals in controlling surface potassium channel numbers. *Science* 291, 316–319.
- [10] Zuzarte M., Rinne S., Schlichthorl G., Schubert A., Daut J., Preisig-Muller R. (2007) A di-acidic sequence motif enhances the surface expression of the potassium channel TASK-3. *Traffic* 8, 1093–1100.
- [11] Barlowe C. (2003) Signals for COPII-dependent export from the ER: what's the ticket out? *Trends Cell Biol.* 13, 295–300.
- [12] Tang W., Ruknudin A., Yang W.P., Shaw S.Y., Knickerbocker A., Kurtz S. (1995) Functional expression of a vertebrate inwardly rectifying K^+ channel in yeast. *Mol. Biol. Cell* 6, 1231–1240.
- [13] Shikano S., Coblitz B., Sun H., Li M. (2005) Genetic isolation of transport signals directing cell surface expression. *Nat. Cell Biol.* 7, 985–992.
- [14] Grishin A., Li H., Levitan E.S., Zaks-Makhina E. (2006) Identification of gamma-aminobutyric acid receptor-interacting factor 1 (TRAK2) as a trafficking factor for the K^+ channel Kir2.1. *J. Biol. Chem.* 281, 30104–30111.
- [15] Yi B.A., Lin Y.F., Jan Y.N., Jan L.Y. (2001) Yeast screen for constitutively active mutant G protein-activated potassium channels. *Neuron* 29, 657–667.
- [16] Kolacna L., Zimmermannova O., Hasenbrink G., Schwarzer S., Ludwig J., Lichtenberg-Frate H. et al. (2005) New phenotypes of functional expression of the mKir2.1 channel in potassium efflux-deficient *Saccharomyces cerevisiae* strains. *Yeast* 22, 1315–1323.
- [17] Holton K.L., Loder M.K., Melikian H.E. (2005) Nonclassical, distinct endocytic signals dictate constitutive and PKC-regulated neurotransmitter transporter internalization. *Nat. Neurosci.* 8, 881–888.
- [18] Gietz R.D., Schiestl R.H. (2007) High-efficiency yeast transformation using the LiAc/SS carrier DNA/PEG method. *Nat. Protoc.* 2, 31–34.
- [19] Kushnirov V.V. (2000) Rapid and reliable protein extraction from yeast. *Yeast* 16, 857–860.
- [20] Bendahhou S., Donaldson M.R., Plaster N.M., Tristani-Firouzi M., Fu Y.H., Ptacek L.J. (2003) Defective potassium channel Kir2.1 trafficking underlies Andersen-Tawil syndrome. *J. Biol. Chem.* 278, 51779–51785.
- [21] Ma D., Tang X.D., Rogers T.B., Welling P.A. (2007) An Andersen-Tawil syndrome mutation in Kir2.1 (V302M) alters the G-loop cytoplasmic K^+ conduction pathway. *J. Biol. Chem.* 282, 5781–5789.
- [22] Ma D., Taneja T.K., Hagen B.M., Kim B.Y., Ortega B., Lederer W.J. et al. (2011) Golgi export of the Kir2.1 channel is driven by a trafficking signal located within its tertiary structure. *Cell* 145, 1102–1115.
- [23] Benatuil L., Perez J.M., Belk J., Hsieh C.M. (2010) An improved yeast transformation method for the generation of very large human antibody libraries. *Protein Eng. Des. Sel.* 23, 155–159.
- [24] Schwarzer S., Kolacna L., Lichtenberg-Frate H., Sychrova H., Ludwig J. (2008) Functional expression of the voltage-gated neuronal mammalian potassium channel rat ether a-go-go1 in yeast. *FEMS Yeast Res.* 8, 405–413.
- [25] Goldstein S.A., Bockenhauer D., O'Kelly I., Zilberberg N. (2001) Potassium leak channels and the KCNK family of two-P-domain subunits. *Nat. Rev. Neurosci.* 2, 175–184.
- [26] Boulkroun S., Samson-Couterie B., Golib-Dzib J.F., Amar L., Plouin P.F., Sibony M. et al. (2011) Aldosterone-producing adenoma formation in the adrenal cortex

- involves expression of stem/progenitor cell markers. *Endocrinology* 152, 4753–4763.
- [27] Pei L., Wiser O., Slavin A., Mu D., Powers S., Jan L.Y. et al. (2003) Oncogenic potential of TASK3 (Kcnk9) depends on K⁺ channel function. *Proc. Natl. Acad. Sci. U.S.A.* 100, 7803–7807.
- [28] Barel O., Shalev S.A., Ofir R., Cohen A., Zlotogora J., Shorer Z. et al. (2008) Maternally inherited Birk Barel mental retardation dysmorphism syndrome caused by a mutation in the genomically imprinted potassium channel KCNK9. *Am. J. Hum. Genet.* 83, 193–199.
- [29] Clarke C.E., Veale E.L., Green P.J., Meadows H.J., Mathie A. (2004) Selective block of the human 2-P domain potassium channel, TASK-3, and the native leak potassium current, IKSO, by zinc. *J. Physiol.* 560, 51–62.
- [30] Zaks-Makhina E., Kim Y., Aizenman E., Levitan E.S. (2004) Novel neuroprotective K⁺ channel inhibitor identified by high-throughput screening in yeast. *Mol. Pharmacol.* 65, 214–219.
- [31] Sannerud R., Marie M., Nizak C., Dale H.A., Pernet-Gallay K., Perez F. et al. (2006) Rab1 defines a novel pathway connecting the pre-Golgi intermediate compartment with the cell periphery. *Mol. Biol. Cell* 17, 1514–1526.
- [32] Kano F., Yamauchi S., Yoshida Y., Watanabe-Takahashi M., Nishikawa K., Nakamura N. et al. (2009) Yip1A regulates the COPI-independent retrograde transport from the Golgi complex to the ER. *J. Cell Sci.* 122, 2218–2227.
- [33] Rao Y., Ruckert C., Saenger W., Haucke V. (2012) The early steps of endocytosis: from cargo selection to membrane deformation. *Eur. J. Cell Biol.* 91, 226–233.
- [34] Declercq J., Meulemans S., Plets E., Creemers J.W. (2012) Internalization of pro-protein convertase PC7 from plasma membrane is mediated by a novel motif. *J. Biol. Chem.* 287, 9052–9060.
- [35] Yancoski J., Sadat M.A., Aksentijevich N., Bernasconi A., Holland S.M., Rosenzweig S.D. (2012) A novel internalization motif regulates human IFN- γ R1 endocytosis. *J. Leukoc. Biol.* 92, 301–308.